The developmental proteome of *Drosophila melanogaster*

Nuria Casas-Vila, Alina Bluhm, Sergi Sayols, et al.

Genome Res. published online April 5, 2017
Access the most recent version at doi:10.1101/gr.213694.116

The developmental proteome of *Drosophila melanogaster*

Nuria Casas-Vila[1,8], Alina Bluhm[1,8], Sergi Sayols[2,8], Nadja Dinges[3], Mario Dejung[4], Tina Altenhein[5], Dennis Kappei[6], Benjamin Altenhein[5,7], Jean-Yves Roignant[3] and Falk Butter[1,9]

[1] Quantitative Proteomics, Institute of Molecular Biology (IMB), Mainz, Germany

[2] Bioinformatics Core Facility, Institute of Molecular Biology (IMB), Mainz, Germany

[3] RNA Epigenetics, Institute of Molecular Biology (IMB), Mainz, Germany

[4] Proteomics Core Facility, Institute of Molecular Biology (IMB), Mainz, Germany

[5] Institute of Genetics, Johannes Gutenberg University (JGU), Mainz, Germany

[6] Cancer Science Institute of Singapore, National University of Singapore (NUS), Singapore

[7] Institute of Zoology, University of Cologne, Cologne, Germany

[8] Equal contribution

[9] To whom correspondence should be addressed: f.butter@imb.de; Institute of Molecular Biology (IMB), Ackermannweg 4, 55128 Mainz

Keywords: *Drosophila melanogaster*, gene regulation, development, embryogenesis, proteomics, systems biology

ABSTRACT

Drosophila melanogaster is a widely used genetic model organism in developmental biology. While this model organism has been intensively studied at RNA level, a comprehensive proteomic study covering the complete life cycle is still missing. Here, we apply label-free quantitative proteomics to explore proteome remodeling across *Drosophila*'s life cycle, resulting in 7,952 proteins, and provide a high temporal-resolved embryogenesis proteome of 5,458 proteins. Our proteome data enabled us to monitor isoform-specific expression of 34 genes during development, to identify the pseudogene Cyp9fpsi as a protein-coding gene and to obtain evidence of 268 small proteins. Moreover, the comparison with available transcriptomic data uncovered examples of poor correlation between mRNA and protein, underscoring the importance of proteomics to study developmental progression. Data integration of our embryogenesis proteome with tissue-specific data revealed spatial and temporal information for further functional studies of yet uncharacterized proteins. Overall, our high resolution proteomes provide a powerful resource and can be explored in detail in our interactive web interface.

INTRODUCTION

Drosophila melanogaster is among the best-described model organisms for development and ageing. During its life cycle, it progresses through well-defined stages including embryo, larva, pupa and adult, undergoing a complete phenotypic metamorphosis (Lawrence 1992). These transitions are based on tightly regulated gene expression at the transcriptional, epigenetic and translational level. Currently, most developmental gene expression studies in *Drosophila* rely on *in situ* hybridization of RNA (Lécuyer et al. 2007; Tomancak et al. 2007), transcriptome analysis using large-scale microarray/RNA-seq data sets (Brown et al. 2014; Chintapalli et al. 2007; Graveley et al. 2011; Kalinka et al. 2010) or a combination of both (Jambor et al. 2015). However, mRNAs are further translated into proteins, which perform the actual cellular functions. It has been shown in multiple species such as *Saccharomyces cerevisiae* (Griffin et al. 2002), *Trypanosoma brucei* (Butter et al. 2013), *Caenorhabditis elegans* (Grün et al. 2014), human (Schwanhäusser et al. 2011) as well as in *Drosophila melanogaster* (Bonaldi et al. 2008)

that transcript levels are only a moderate predictor for protein expression as they do not account for posttranscriptional processes such as translational regulation or protein stability (Liu et al. 2016; Vogel and Marcotte 2012). Recently, this has also been addressed with a developmental perspective in *Caenorhabditis elegans* (Grün et al. 2014), *Xenopus laevis* (Peshkin et al. 2015) and *Trypanosoma brucei* (Dejung et al. 2016), but not yet in *Drosophila*.

The number of fly proteins with available antibodies increased in the last decade from around 450 (Adams et al. 2000) to 1,586 (listed in FlyBase version 6.01), but still covers only a small fraction of expressed genes. To accelerate protein studies in *Drosophila*, several tagging strategies were devised. Around 100 genes have been fused with a GFP using piggyBac transposition (Morin et al. 2001) and 400 GFP-tagged fly lines have been established using MiMICs (Minos Mediated Integration Cassette) to permit systematic protein investigations (Nagarkar-Jaiswal et al. 2015). In an alternative approach, BAC TransgeneOmics allowed the creation of 880 lines and the systematic study of 207 GFP-tagged fly proteins (Sarov et al. 2016). In principle, all protein-coding genes can be investigated, but this requires the establishment of a line for each protein. Additionally, a putative caveat of tagging strategies is altered protein behavior like mislocalization, changes in protein stability or a dominant negative regulatory effect (Margolin 2012).

The fruit fly is one of the model species investigated by modENCODE (The modENCODE consortium et al. 2010) and thus several large data sets are available for mapping histone modifications (Kharchenko et al. 2011), global RNA levels during development (Graveley et al. 2011) and tissue-specific splicing (Brown et al. 2014). In contrast, proteomic studies in *Drosophila* have been restricted to certain developmental stages. For example, changes in the proteome during ageing from eclosure to 60 days old flies (Sowell et al. 2007), the adult itself (Sury et al. 2010; Xing et al. 2014), larva and pupa (Chang et al. 2013), the embryo (Fabre et al. 2016) and the oocyte-to-embryo transition (Kronja et al. 2014) have been investigated. However, these studies have relatively low proteome coverage (around 2,000 proteins), do not cover the complete developmental process and are not directly comparable because of technical differences.

Applying label-free quantitative proteomics (Cox et al. 2014), we here measured protein expression throughout the *Drosophila* life cycle with a coverage of 7,952 proteins to provide insight into proteome remodeling. With embryogenesis being a focus in *Drosophila* developmental studies, we amended the life cycle proteome with an embryogenesis proteome of 5,458 proteins with high temporal resolution. Finally, data integration with tissue-specific (Lécuyer et al. 2007) and developmental transcriptomic studies (Graveley et al. 2011) allows investigating the importance of spatial and translational regulation.

RESULTS

Proteomics screen of the life cycle

We collected whole animal samples at 15 representative time points during the *Drosophila* life cycle (Fig. 1A). The embryonic time points were chosen according to major stages of embryonic development: prior to zygotic gene activation (0-2h, E02), gastrulation (4-6h, E06), organogenesis (10-12h, E10) and the late stages of embryogenesis (18-20h, E20). For larva, the three different instar larva (L1, L2 and early L3) and a late stage (L3 crawling larva) were examined. Pupae were collected daily starting with the white pupa and, for adults, the virgin males and females (up to 4h after eclosure) as well as one week old animals of each sex were chosen. All samples were collected as biological quadruplicates and processed by mechanical disruption with a universal protein extraction protocol. For each replicate, a five hour mass spectrometry (MS) run was used, resulting in 340 hours of measurement (68 MS runs). We searched the resulting 8 million MS/MS spectra against a *Saccharomyces cerevisiae* and *Drosophila melanogaster* database using the MaxQuant software suite (Cox and Mann 2008). Overall, we identified 9,627 protein groups (a protein group contains proteins indistinguishable by the peptides that were identified) with 144,067 unique peptide sequences at a FDR<0.01. This number includes 1,078 yeast and 8,549 *Drosophila* protein groups (Supplemental Fig. S1A). The identification of yeast proteins is nearly exclusively restricted to the larval stages where it is a food source (Supplemental Fig. S1B). The number of 8,549 identified fly proteins is

comparable to a previous in-depth measurement of multiple sources of *Drosophila* material reaching 9,124 proteins (Brunner et al. 2007). After filtering for robust detection in at least two replicates of any time point, we performed our subsequent analysis on a set of 7,952 protein groups (Fig. 1B and Supplemental Table S1).

Developmental processes are tightly regulated and thus highly reproducible in each organism. Nevertheless, to visualize biological variability of this process, we performed correlation and principal component analysis (PCA). To increase quantitation reliability, all label-free quantitation (LFQ) values were solely based on unique peptide intensities for each protein group. Despite that our replicates are originating from different egg-laying events, being processed independently and measured several days apart on the mass spectrometer, we find a very high correlation within the time points (R = 0.84-0.98) (Supplemental Fig. S1C) and clear formation of clusters in PCA (Fig. 1C). These findings demonstrate a very high reproducibility of our experimental conditions from the biological system to the mass spectrometry measurement.

Core proteome and protein expression dynamics

To identify a core proteome, i.e. proteins detected at all stages of development, we grouped the proteins according to their presence in the four major stages of the life cycle (Fig. 2A). We found 4,627 proteins groups, more than half of our proteome, to be detectable in all stages. To obtain an overview of the functionality of these continuously expressed proteins, we performed gene ontology (GO) annotation enrichment analysis and reduced the GO term complexity to uncover major descriptors (Fig. 2B). As expected, our core proteome is enriched for metabolic and cellular processes describing the basic activities of any cellular system, exemplified by covering all known proteins for such essential processes as tRNA aminoacetylation, endosome transport via multivesicular body sorting pathway, cell junction maintenance, nuclear pore organization and ribosome assembly (Fig. 2B and Supplemental Fig. S2A, Supplemental Table S2). We also analyzed developmental expression dynamics for all proteins with an averaged abundance above the detection limit, $\log_2$ LFQ intensity >25 (Fig. 2C, Supplemental Table S3). We additionally applied a Gini coefficient filter of 0.1, which divided our proteome into 1,386 stably

expressed proteins throughout life cycle and 1,978 differentially expressed proteins. Consistent with a previous developmental study in *Xenopus*, we see that the dynamicity decreases with protein abundance (Peshkin et al. 2015) (Fig. 2C). We show examples of highly dynamic and stably expressed proteins (Fig. 2D, Supplemental Fig. S2D). The stable proteins include the widely accepted loading controls: tubulins, actins, heat-shock proteins, Gapdh1, Gapdh2 and Vinculin.

Developmental expression profiles of highly abundant proteins

We first characterized the 100 most abundant proteins per stage, comprising around 10% of the total protein mass (Supplemental Table S1). Among proteins with the highest LFQ values, we find ribosomal proteins, being especially prevalent in the top 100 list during embryogenesis, a phase of rapid cell proliferation. The fly uses different storage proteins at specific developmental stages: yolk proteins (Yp1, Yp2 and Yp3) in embryogenesis and Lsp proteins whose protein abundance rises drastically in L3. Among these highly abundant proteins there are several preliminary annotated genes that are not further characterized. CG1850, representing the most abundant protein in the pupal stage, shares a small stretch of similarity to the cuticular protein Cpr72Eb (BLAST E-value: 0.019, Supplemental Fig. S2B). Interestingly, some other highly expressed computed genes (CG) also show similar protein expression patterns to well-studied cuticular proteins like Cpr72Ea (CG1850 and CG13023), Cpr64Aa and Cpr64Ac (CG34461 and CG42323) and Cpr66D (CG16886 and CG30101). While thus far we looked at the most highly expressed 100 proteins, our proteome can be interrogated to reveal the temporal expression pattern of any quantified protein.

Proteome remodeling throughout the life cycle

Our proteome covers a dynamic range of more than 6 orders of magnitude showing expression changes of individual proteins of more than 100,000 fold (Supplemental Fig. S2C). We interrogated our data set for stage-specific proteins by applying ANOVA (FDR<0.01) on the $\log_2$ LFQ values (Fig. 3A). The majority of these 1,535 differentially regulated protein groups are found in adult flies (556), followed by embryos (473), pupae (317) and larvae (189). To connect

the proteome differences to stage-specific biological functions, we performed GO enrichment analysis on clustered protein expression profiles (Fig. 3A, Supplemental Tables S4 and S5). The most enriched GO terms during embryogenesis include mitotic cell cycle regulation and nuclear division represented by cyclins (CycE, CycA, CycB) and developmental kinases, such as Loki (Lok), Greatwall (Gwl) and Grapes (Grp). By this clustering, we were able to separate an early and late embryogenesis phase (Fig. 3B). The early phase (0-6h) is characterized by high expression of proteins involved in cytoskeleton organization (Dgt4, AlphaTub67C and GammaTub37C), microtubule binding proteins (Mars and Wee Augmin (Wac)) as well as the classical examples Bicaudal C (BicC) and Cup, important in translational regulation of the *oskar* mRNA. In contrast, proteins involved in tissue morphogenesis such as Bazooka (Baz), Fat (Ft), Ribbon (Rib) and Tramtrack (Ttk) are upregulated in later phases (12-20h). Stage-specific proteins in larvae and pupae include expected structural constituents of the chitin-based cuticle: Lcp, Tweedle (Twd) and cuticular proteins. Intriguingly, several proteins that are highly upregulated only at a single pupal stage, like CG13376, CG13082 and CG42449, are poorly characterized (Fig. 3B and Supplemental Fig. S3A). In the adult, odorant-binding proteins (Obp83b and Obp57a), proteins involved in light perception and phototransduction (Arr1 and Arr2) and the retinal degeneration protein A (RdgA) show strong expression, consistent with the adult fly having a fully developed light sensory system. Also proteins involved in muscle contraction like flightin (Fln) and Eaat1, increase their expression 100-fold in adult stages (Fig. 3B).

Overall, our data is in agreement with previously published studies and connects protein expression with well-described morphological changes during *Drosophila* development. Therefore, our screen defines the developmental stage to study molecular or phenotypic effects of yet uncharacterized proteins. All protein profiles can be interrogated using the interactive web interface (http://www.butterlab.org/flydev).

Developmentally regulated functions: ecdysone-induced proteins and cuticle formation

The regulation of molting by endogenous 20-hydroxyecdysone (20E) is a prototype example of hormonal gene regulation pathways in insects (Yamanaka et al. 2013). Previous microarray studies focused on 20E-induced gene regulation of mRNA transcripts between L3 larval stage and 12h after puparium formation (Beckstead et al. 2005; Gonsalves et al. 2011). However, for the ecdysone-induced gene family 71E (*Eig71E*), we find intriguing differences between the expression profiles of mRNA and protein in pupae. Messenger RNA expression is detectable in three different waves: *Eig71Ee* spikes at L3c, another group represented by *Eig71Ed* at P1 and a later group represented by *Eig71Ek* at P2 (Graveley et al. 2011) (Fig. 3D and Supplemental Fig. S3B). While the mRNA is detectable only in early pupal stages, the corresponding Eig71E proteins show prolonged high expression levels until P5 (Fig. 3C and 3D). Likewise, second puff genes display a similar transcriptome versus proteome pattern. A 1000-fold upregulation of glue proteins (Sgs5, Sgs7 and Sgs8) at late L3 concordant to the detection of their mRNA in a narrow window of circa 24h between crawling L3 and P1 (Beckstead et al. 2005), is followed by the presence of the protein in all pupal stages (Fig. 3D and Supplemental Fig. S3C). Our data shows that for selected puff proteins, protein stability is the major determinant of their expression patterns during development. In contrast, in a high number of cases, we detect the protein at a single time point while the RNA is detectable at multiple time points (Fig. 3E). In the aforementioned cases, protein levels cannot be directly predicted by transcriptomics, which demonstrates the necessity of proteome data for studying fly development.

Comparison of gender-specific protein patterns in adult flies

Gender-specific proteins are of high interest and have already been investigated by several proteomics studies (Dorus et al. 2006; Sury et al. 2010; Takemori and Yamamoto 2009; Wasbrough et al. 2010). To benchmark our label-free quantitative approach we compared our adult time point to the published SILAC data set (Sury et al. 2010) and found a high overlap of gender-specific proteins (R=0.84, Supplemental Fig. S4A), showing that our developmental proteome recapitulates previous studies that are more specialized. To identify gender-specific proteins, we defined a 4-fold expression difference with a p-value below 0.01 between male and

female flies (one week old) and found 308 male- and 374 female-specific proteins (Fig. 4A, Supplemental Table S6). The 308 male proteins include Tektin-A and Tektin-C as sperm-specific flagellar proteins (Amos 2008), several less characterized genes known to be expressed in fly testes and seminal vesicles (Dorus et al. 2006; Takemori and Yamamoto 2009) and some proteins functioning in male development like Lectin-46Ca, Lectin46Cb and Lectin-30A. For some proteins like Hsp60B, Hsp60C, the male fertility factor Kl-5 as well as Aquarius (Aqus) and Antares (Antr), an essential role in sperm development or sperm storage has already been demonstrated. The list of 374 female-specific proteins include vitelline membrane (Vm32E) and chorion proteins (Cp15, Cp18, Cp36), which are important for eggshell assembly, the vitellogenins (Yp1, Yp2 and Yp3) and the fatty acid desaturase Fad2.

Additionally, our developmental proteome allows the investigation of young flies, which were collected as virgins within 4h after eclosure (Supplemental Table S7). The majority of proteins are equally expressed in both genders (Supplemental Fig. S4B). While we detect only 21 female-specific proteins in young flies, there are 155 proteins with higher expression in its male counterpart (Fig. 4B, Supplemental Fig. S4C and S4D). In agreement with this observation, a previous transcriptomic study showed upregulation of genes in female flies after mating, suggestively triggered by sperm and seminal fluid proteins (McGraw et al. 2008). In contrast, the majority of male-specific proteins is already present in young male flies prior to mating (Fig. 4B, Supplemental Fig. S4D). Interestingly, the only two proteins with more than 30-fold upregulation in virgin females compared males are not characterized: CG31862 and CG12288. Noteworthy, CG31862 is found in P5 and shows continuously high protein level, while its RNA expression is restricted to the late pupal phase (Fig. 4C).

Maternally loaded proteins

While there is ample knowledge about maternally loaded RNA in *Drosophila* embryos (Tadros and Lipshitz 2005), no systematic analysis for maternally loaded proteins has been conducted yet. We interrogated our data for proteins enriched during embryogenesis whose RNA levels were higher in adult females compared to adult males. Among this subset of likely maternally

loaded material should be candidates that have a functional importance during early development. In most cases, protein and mRNA are present in 2h old embryos, suggesting that both are maternally loaded (Fig. 4D and Supplemental Table S8). These include well-known examples such as Oskar (Osk), String (Stg), Piwi, Aubergine (Aub), Extra sexcombs (Esc), Dorsal (Dl), Mothers against dpp (Mad) and Swallow (Swa) (Chao et al. 1991; Edgar and Datar 1996; Luschnig et al. 2004; Mani et al. 2014; Simmons et al. 2010). However, also yet undescribed candidates like CG11674, CG5568, CG17018, CG15047, Zpg, GammaTub37C and Tosca found in this set represent interesting candidates with a putative role in oogenesis and early embryogenesis. In order to investigate potential germline-specific functions of these candidates we performed RNAi mediated-knockdown using the driver *nanos*-GAL4 and specific transgenic lines expressing double–stranded RNA from inverted repeats (shRNAs). Germline-specific expression of two independent shRNAs targeting CG17018 RNA revealed drastic effects on the embryonic hatching rate. While the number of laid eggs was unaffected (Supplemental Fig. S4E), hatching was reduced by almost 80% (Fig. 4E). Besides, approximately 30% of unhatched eggs displayed defective dorsal appendages that are fused (Fig. 4F). Cuticle preparations showed that *CG17018* knockdown embryos miss the denticle belts, revealing an absence of patterning at early stages (Fig. 4G). To note, *CG17018* knockdown ovaries were indistinguishable from wild type ones, as we could not detect any obvious morphological or differentiation defects (Supplemental Fig. S4F). Taken together, our findings imply a critical role of CG17018 during early embryogenesis.

Furthermore, our proteomic data set allows a comprehensive classification of maternally loaded proteins when the RNA is not present. The most prominent proteins include the major egg yolk vitellogenins (Yp1, Yp2 and Yp3), Dec-1, Cp36 and Cp7Fb as part of the chorion, the oxidoreductase family member CG12398 for which a role in vitelline membrane formation has been previously suggested (Fakhouri et al. 2006), the serine protease Nudel (Ndl), the sensor protein Obp19c, the female-specific protein Fit as well as two uncharacterized candidates, CG14309 and CG14834 (Fig. 4D and Supplemental Table S8).

Small proteins in the developmental proteome

Recently, there has been an increased interest in small proteins and translated small ORF (smORF) with up to 100 amino acids (Ramamurthi and Storz 2014) as their protein coding potential is difficult to assess bioinformatically (Ladoukakis et al. 2011). These small proteins localize to specific subcellular compartments and perform cellular functions as any other protein (Magny et al. 2013). Our data set detects 268 small proteins (Fig. 5A) of which 84% have two or more unique peptides and temporal expression information (Supplemental Fig. S5A and Supplemental Table S1). This number is similar to a previous investigation using ribosome profiling (Aspden et al. 2014), demonstrating that mass spectrometry-based proteomics is *on par* with next generation sequencing approaches to detect translation of small proteins.

Peptides originating from non-coding regions of the genome

Peptides originating from putative non-coding regions have been reported in diverse organisms. Therefore, we re-analyzed our data including ncRNA sequences from FlyBase, which we *in silico* translated for open reading frames of at least 20 amino acids. Overall, we identified 29 putative proteins that unambiguously map to non-translated transcripts at a FDR<0.01 (Supplemental Table S9). Due to short open reading frames of these small proteins, we usually detect a single peptide per transcript. However, only two of these ncRNA-derived peptides showed a good MS2 fragmentation pattern and were independently identified with more than 10 different MS/MS spectra in several replicates and time points. One of these, FBtr0340701 has also been found in a control experiment using human cell lysate (data not shown), classifying it as a false positive identification originating from a contaminant. The only remaining peptide with strong evidence of identification matches to *CR43476* (Fig. 5B).

Other genes classified as non-expressed are pseudogenes. These genes have mutations in their promoter regions or other functional elements that make their expression unlikely (Harrison et al. 2003). We checked for protein evidences of the 2,902 reported pseudogenes (FlyBase 6.01), and found 9 protein groups in our dataset to include peptides unambiguously mapping to pseudogenes. Whereas most of these proteins are represented by a single peptide

(Supplemental Table S10), the most prominent hit, FBtr0082602 encoding Cyp9f3psi, is supported by 23 peptides including 5 unique sequences. The measured peptides match to the N-terminal and C-terminal regions, demonstrating that the complete pseudogene is most likely translated (Fig. 5C). Furthermore, Cyp9f3psi and Cyp9f2 present distinct expression patterns, further indicating that despite their close genomic vicinity they are differently regulated during development (Supplemental Fig. S5B).

Despite an extremely low expression of peptides originating from ncRNA transcripts, only very few detected peptides map to non-coding regions of the genome, illustrating a low false discovery rate in our screen and a carefully curated gene annotation of the *Drosophila melanogaster* genome (Matthews et al. 2015).

Highly temporal-resolved embryogenesis proteome

Being intensely studied, we were particularly interested in proteome changes during embryogenesis. To investigate the process in a high time-resolved and systematic manner, we collected whole embryos at narrow intervals: every single hour after egg laying for up to 6h and then every two hours until 20h (Fig. 6A). These 14 time points were also measured in four independent biological replicates to account for technical, biological and environmental variation. To control for our collections, we staged embryos of selected time points by morphology and Engrailed antibody staining (Campos-Ortega and Hartenstein 1997) (Supplemental Fig. S6A). Protein expression levels were determined using label-free quantitation based on unique peptides provided by MaxLFQ (Cox et al. 2014). We detected 6,487 expressed protein groups of which 5,458 were quantified in at least two replicates of any time point (Supplemental Table S11). PCA revealed that embryo stages correlate well with our collected time points (R=0.93), showing a developmental progression through embryogenesis (Fig. 6A, Supplemental Fig. S6C). Noteworthy, all four independent biological replicates show very high reproducibility (R=0.92-0.96) (Supplemental Fig. S6B and S6C). We also validated the expression profiles of seven protein by immunostaining with antibodies against endogenous proteins (Fig. 6C and Supplemental Fig. S6D).

Expression profiles during embryogenesis

We analyzed the time course data using a multivariate empirical Bayes approach and identified 1,644 protein groups with differential expression during embryogenesis (Fig. 6B). To obtain a functional overview on the embryogenesis process, we performed GO enrichment analysis on this set of differentially expressed proteins. Based on this analysis, we observed enrichment of terms related to very early embryogenesis cellular processes (0-1h), such as zygotic determination of anterior/posterior axis and syncytial blastoderm mitotic cell cycle (Fig. 6D). Additionally, proteins involved in ribosome biogenesis upregulate at 2h to initiate active translation concomitant with zygotic gene activation (ZGA) starting at 2h. We also noted high enrichment of proteins involved in cell cycle and cytoskeleton organization during early phases of embryogenesis (2-3h). While proteins involved in nervous system development are highly present at 3h, muscle structure development proteins are more prominent later in embryogenesis at 14h.

As an alternative approach to analyze the data, we automatically clustered the differentially expressed proteins with similar temporal profiles, resulting in 70 distinct clusters and performed GO enrichment analysis on these clusters (Fig. 6E, Supplemental Table S12 and S13). As a result, the known embryonic developmental program can be followed by temporal alignment of individual clusters (Fig. 6E), possibly hinting at putative functions of not yet characterized proteins.

Integrating the developmental proteome and spatial expression

To integrate spatial information, we fused our proteome profiles with tissue-specific RNA expression data from fluorescence *in situ* hybridizations (Lecuyer et al., 2007). We chose muscle development to highlight the value provided by the merged data. In the muscle-specific clusters (Fig. 6F, Supplemental Table S14 and S15), we noted upregulation of proteins involved in muscle development such as Mlc2, Mp20 and Mlp60A (Sandmann et al. 2006) at 14h. Later in embryogenesis (20h), we found high expression of Eaat1 and EcR, which control muscle contraction at larval stages. Furthermore, this data integration allowed us to identify similarly

expressed, not yet characterized proteins (CG1674, CG6040 and CG15022), shown to localize in muscle tissue, suggesting a role in muscle development. In order to test this hypothesis, we performed RNAi mediated-knockdown of two candidates. Remarkably, mesodermal knockdown of either *CG1674* or *CG6040* severely affects locomotion behavior of adult flies (Fig. 6G and Supplemental Fig. S6E). Likewise, the complete *CG6040* loss-of-function produces viable flies that display similar climbing defects, confirming the specificity of the RNAi phenotype. Importantly, neuronal knockdown of both genes did not impair locomotion performance, supporting their muscle-specific functions. We next performed *in situ* hybridization on embryos and observed a strong enrichment of *CG1674* mRNA in muscle tissue, more specifically in somatic and pharyngeal muscles, whereas *CG6040* exhibits moderate ubiquitous expression (Supplemental Fig. S6F). Altogether, our findings strongly suggest a muscular function for *CG1674* and *CG6040*. However, further investigations will be required to investigate their specific role in muscle development.

Alternatively, other tissue data can be inspected for biological insights. The analysis of the central nervous system (CNS) revealed an upregulation of proteins involved in neural development (Roughest (Rst), Smooth (Sm) and Erect wing (Ewg)) at 8-12h and in synapse organization and axon ensheathment (Ank2 and Wrapper) at 14h (Fig. 6F, Supplemental Table S14 and S15). Likewise, all 21 tissue clusters can be examined in our web interface.

Comparing transcriptome and proteome to study translational delay

We compared our embryogenesis proteome with the transcriptome generated as part of the modENCODE project (Graveley et al. 2011). In agreement with the transcriptome analysis, we found that the general protein complexity is increased during embryogenesis (Fig. 7A and Supplemental Fig. S7A). Similar to a previous study in yeast (Fournier et al. 2010), we found only a moderate correlation (maximum R=0.5) between transcriptome and proteome and noted that the best correlation is non-synchronous, showing a 4-5 hours proteome delay (Fig. 7B).

By multidimensional scaling followed by clustering, we sub-grouped the RNA/protein expression profiles into 6 clusters (Fig. 7C, Supplemental Table S16). In the majority of cases, the mRNA is

more abundant at early time points, while the protein expression peaks at later stages. Except for cluster 1, the remaining clusters illustrate different behavior of RNA and protein during embryogenesis. We observed a temporal proteome delay in clusters 5 and 6: while the RNA expression peaks around 7h, proteins steadily upregulate later in embryogenesis, putatively due to translational control mechanisms (Fig. 7C).

Quantification of protein isoforms during embryogenesis

As distinct protein isoforms may show differential developmental regulation, we mined our proteomic data for protein isoforms. We found 34 genes with various quantified isoforms, some of them showing differential expression such as *lola*, *mod(mdg)4* and *Rtnl1* (Fig. 7D and Supplemental Fig. S7B). We further validated our isoform quantitation by immunoblotting following the expression of Lola- RAA/RI (also known as Lola-K) (Giniger et al. 1994). While Lola- RAA/RI is highly expressed at 20h (Fig. 7E), its mRNA shows an expression peak at 14h shown by *in situ* hybridization (Fig. 7F). This underscores again the importance of a developmental proteome as an addition to transcriptomic studies.

DISCUSSION

We generated high quality proteome data sets for embryogenesis and the full life cycle of *Drosophila melanogaster* that close the gap for systematic developmental investigation of protein expression. Both proteomes cover nearly 8,000 and 5,500 protein groups during life cycle and embryogenesis, respectively, accounting for at least one third of annotated *Drosophila* genes. However, while these two data sets are larger than previous ones, they are not complete. Especially low abundant proteins or proteins that are highly expressed in a restricted number of small tissues will likely not be present in our proteomes. Thus, a not quantified protein can either be absent in this stage or expressed below our limit of detection (LOD) enforced by the mass spectrometry measurement. Nevertheless, these large-scale data sets allow us to assess the developmental expression of proteins and protein isoforms, report

maternally provided proteins, validate small proteins (≤100 amino acids), identify Cyp9f3psi as an expressed protein-coding gene and describe peptides originating from non-coding regions.

We scored significantly developmental-regulated protein groups: 1,535 for the whole life cycle and 1,644 for embryogenesis. Nearly half of them are not in-depth characterized suggesting a large area of developmental gene regulation still to be discovered.

We used our data to follow the well-characterized regulation by the hormone ecdysone at a protein level. This revealed intriguing differences to previously reported transcriptome analysis (Beckstead et al. 2005; Gonsalves et al. 2011). For several ecdysone-induced genes, the protein abundance relies on protein stability rather than the presence of RNA transcripts. Overall, transcript abundance and protein levels correlate only modestly. The same observation holds true even considering the temporal delay between transcript and protein expression. The temporal difference in RNA and protein expression needs to be taken into account when studying phenotypic differences of protein-coding genes using mRNA as a proxy.

As previous transcriptomic studies reported maternally loaded RNAs, our proteomic data enables systematic identification of maternally provided proteins. Here we catalogue not yet reported maternally loaded proteins such as CG14309, CG14834 and CG12398, whose functions in early development need further investigations. For instance, the knockdown of the maternally loaded protein CG17018 results in a severe defect in embryo development.

To gain further insights, we complemented our data sets with other available published data. For example, to deconvolute tissue-specific expression information, we merged our embryogenesis proteome to RNA *in situ* hybridization data (Lécuyer et al. 2007). This allowed us to pinpoint individual proteins showing tissue-specific developmental regulation, as exemplified with the impaired muscular phenotypes of *CG1674* and *CG1640* knockdown lines. Additionally, this analysis can be extended to other tissues to uncover currently unknown proteins, which might play an essential role in the development of a specific tissue. This underscores the power to combine available high-quality *Drosophila* data sets to achieve a

more holistic model for developmental gene regulation. While we highlight several interesting results, the entire data sets are available at http://www.butterlab.org/flydev.

METHODS

Collection of embryos, larvae, pupae and adult flies

Population cages of wild type Oregon R flies containing only fertilized females were maintained at 25°C. For the whole life cycle comparative analysis, embryos were collected from cages on agar apple juice plates in 2 hour laying time windows and processed immediately (0-2h) or aged at 25°C for the required time (4-6h, 10-12h, 18-20h). Early larval collections were performed from embryo plates whereas crawling larvae and pupae stages were collected directly from flasks at indicated time points. Virgin young flies within 4h after eclosure were collected separately for males and females, as well as one week old flies (adult flies). For the time course analysis, embryos were collected on apple juice agar plates in 30 min laying time windows, processed immediately (0h time point) or aged at 25°C for the required time. All samples were mechanically lysed prior to mass spectrometry sample preparation (see supplemental materials for detailed descriptions).

Mass spectrometry measurement and label-free analysis

Peptides were separated by nanoflow liquid chromatography on an EASY-nLC 1000 system (Thermo) coupled to a Q Exactive Plus mass spectrometer (Thermo). Separation was achieved by a 25 cm capillary (New Objective) packed in-house with ReproSil-Pur C18-AQ 1.9 µm resin (Dr. Maisch). Peptides were separated chromatographically by a 280 min gradient from 2% to 40% acetonitrile in 0.5% formic acid with a flow rate of 200 nl/min. Spray voltage was set between 2.4-2.6 kV. The instrument was operated in data-dependent mode (DDA) performing a top15 MS/MS per MS full scan. Isotope patterns with unassigned and charge state 1 were excluded. MS scans were conducted with 70,000 and MS/MS scans with 17,500 resolution. The raw measurement files were analyzed with MaxQuant 1.5.2.8 standard settings except LFQ

(Cox et al., 2014) and match between run options were activated as well as quantitation was performed on unique peptides only. The raw data was searched against the translated ENSEMBL transcript databases (release 79) of *D. melanogaster* (30,362 translated entries) and the *S. cerevisiae* protein database (6,692 entries). Known contaminants, protein groups only identified by site and reverse hits of the MaxQuant results were removed. In the life cycle data set, the imputation was performed in two distinct ways for proteins with a measured intensity (raw) missing an LFQ intensity or proteins with no intensity value. In the first case, values were imputed from a normal distribution with a mean value shifted by -0.6 from the mean value of all measured LFQ intensities and half of the standard deviation. In contrast, proteins with no intensity value were replaced with the smallest measured value in the set. For the embryo time course, missing values were drawn from a distribution calculated with the logspline R package (Kooperberg 2016). For cases where 3 or more replicates were measured, the mean of the measured replicates was used as the mean parameter of the distribution. Otherwise, the average of the two neighboring time points was used. In cases of no measured values in neighboring time points, or for proteins measured only in 1 replicate with no surrounding values, a fixed value of 22.5 close to the LOD was used.

Bioinformatics analysis

Significant changes during the lifecycle were calculated by analysis of variance (ANOVA), flagging stage-specific proteins those with FDR<0.01 (Benjamini-Hochberg-procedure) and present in either one unique stage or differing in one stage compared to the rest ($\log_2$ LFQ FC>4 in all stages, allowing only one not fulfilling the condition). The effect of the differences was assessed calculating Cohen's effect size and the Tukey HSD post-hoc test. The Gini ratio was used to measure the stability of protein abundance throughout time. Automatic clustering of genes and samples was performed using Affinity Propagation (Frey et al 2007) on the significant proteins, taking negative squared Euclidean distances as a measure of similarity. The goodness of the clusters was assessed from the Silhouette information according to the given clustering. Gene set enrichment analysis (GSEA) was done in R (R core team 2017), followed

by a strategy of scoring similar (redundant) terms calculating the information content (IC) between two terms. Results were presented as a treemap or a scatterplot of terms clustered based on the first 2 components of a PCA of the IC similarity scores. For the embryo development significant changes of protein abundance along the time course was assessed. FPKM levels for FlyBase 5.12 Transcripts from short poly(A)+ RNA-seq (Graveley et al. 2011) and localization data from http://fly-fish.ccbr.utoronto.ca were integrated with our proteome data.

DATA ACCESS

The mass spectrometry raw data from this study have been submitted to the ProteomeXchange (http://www.proteomexchange.org) under the data set identifier PXD005691 (life cycle) and PXD005713 (embryogenesis).

DISCLOSURE DECLARATION

The authors declare that there is no conflict of interest.

ACKNOWLEDGEMENT

We thank Junaid Akhtar for training as well as Marion Scheibe, Anja Freiwald and Christian Berger for critical reading of the manuscript. Antibodies were obtained from the Developmental Studies Hybridoma Bank, created by the NICHD of the NIH or kindly provided by Christian Berger. We acknowledge support of the Zentrum für Datenverarbeitung (ZDV) at the University of Mainz in hosting the web application. The study was partly funded by the Rhineland Palatinate Forschungsschwerpunkt GeneRED (Gene Regulation in Evolution and Development). DK is supported by the National Research Foundation Singapore and the Singapore Ministry of Education under its Research Centres of Excellence initiative.

REFERENCES

Adams MD, Celniker SE, Holt RA, Evans CA, Gocayne JD, Amanatides PG, Scherer SE, Li PW, Hoskins RA, Galle RF, et al. 2000. The genome sequence of *Drosophila* melanogaster, *Science* **287:** 2185–2195.

Amos LA. 2008. The tektin family of microtubule-stabilizing proteins, *Genome Biol* **9:** 229.

Aspden JL, Eyre-Walker YC, Phillips RJ, Amin U, Mumtaz MAS, Brocard M, Couso J-P. 2014. Extensive translation of small Open Reading Frames revealed by Poly-Ribo-Seq, *Elife* **3:** e03528.

Bahadorani S, Hilliker AJ. 2008. Antioxidants cannot suppress the lethal phenotype of a *Drosophila* melanogaster model of Huntington's disease, *Genome* **51:** 392–395.

Beckstead RB, Lam G, Thummel CS. 2005. The genomic response to 20-hydroxyecdysone at the onset of *Drosophila* metamorphosis, *Genome Biol* **6:** R99.

Bonaldi T, Straub T, Cox J, Kumar C, Becker PB, Mann M. 2008. Combined use of RNAi and quantitative proteomics to study gene function in *Drosophila*, *Mol Cell* **31:** 762–772.

Brown JB, Boley N, Eisman R, May GE, Stoiber MH, Duff MO, Booth BW, Wen J, Park S, Suzuki AM, et al. 2014. Diversity and dynamics of the *Drosophila* transcriptome, *Nature* **512:** 393–399.

Brunner E, Ahrens CH, Mohanty S, Baetschmann H, Loevenich S, Potthast F, Deutsch EW, Panse C, Lichtenberg U de, Rinner O, et al. 2007. A high-quality catalog of the *Drosophila* melanogaster proteome, *Nat Biotechnol* **25:** 576–583.

Butter F, Bucerius F, Michel M, Cicova Z, Mann M, Janzen CJ. 2013. Comparative proteomics of two life cycle stages of stable isotope-labeled Trypanosoma brucei reveals novel components of the parasite's host adaptation machinery, *Mol Cell Proteomics* **12:** 172–179.

Campos-Ortega JA, Hartenstein V. 1997. *The embryonic development of Drosophila melanogaster,* 2nd edn. Springer, Berlin, London.

Chang YC, Tang HW, Liang SY, Pu TH, Meng TC, Khoo KH, Chen GC. 2013. Evaluation of Drosophila metabolic labeling strategies for in vivo quantitative proteomic analyses with applications to early pupa formation and amino acid starvation, *J Proteome Res* **3:** 2138-2150.

Chao YC, Donahue KM, Pokrywka NJ, Stephenson EC. 1991. Sequence of swallow, a gene required for the localization of bicoid message in *Drosophila* eggs, *Dev Genet* **12:** 333–341.

Chintapalli VR, Wang J, Dow JAT. 2007. Using FlyAtlas to identify better *Drosophila* melanogaster models of human disease, *Nat Genet* **39:** 715–720.

Cox J, Hein MY, Luber CA, Paron I, Nagaraj N, Mann M. 2014. Accurate proteome-wide label-free quantification by delayed normalization and maximal peptide ratio extraction, termed MaxLFQ, *Mol Cell Proteomics* **13:** 2513–2526.

Cox J, Mann M. 2008. MaxQuant enables high peptide identification rates, individualized p.p.b.-range mass accuracies and proteome-wide protein quantification, *Nat Biotechnol* **26:** 1367–1372.

Dejung M, Subota I, Bucerius F, Dindar G, Freiwald A, Engstler M, Boshart M, Butter F, Janzen CJ. 2016. Quantitative Proteomics Uncovers Novel Factors Involved in Developmental Differentiation of Trypanosoma brucei, *PLoS Pathog* **12:** e1005439.

Dorus S, Busby SA, Gerike U, Shabanowitz J, Hunt DF, Karr TL. 2006. Genomic and functional evolution of the *Drosophila* melanogaster sperm proteome, *Nat Genet* **38:** 1440–1445.

Edgar BA, Datar SA. 1996. Zygotic degradation of two maternal Cdc25 mRNAs terminates *Drosophila*'s early cell cycle program, *Genes Dev* **10:** 1966–1977.

Fabre B, Korona D, Groen A, Vowinckel J, Gatto L, Deery MJ, Ralser M, Russell S, Lilley KS. 2016. nalysis of Drosophila melanogaster proteome dynamics during embryonic development by a combination of label-free proteomics approaches, *Proteomics* **16:** 2068-2080.

Fakhouri M, Elalayli M, Sherling D, Hall JD, Miller E, Sun X, Wells L, LeMosy EK. 2006. Minor proteins and enzymes of the *Drosophila* eggshell matrix, *Dev Biol* **293:** 127–141.

Fournier ML, Paulson A, Pavelka N, Mosley AL, Gaudenz K, Bradford WD, Glynn E, Li H, Sardiu ME, Fleharty B, et al. 2010. Delayed correlation of mRNA and protein expression in rapamycin-treated cells and a role for Ggc1 in cellular sensitivity to rapamycin, *Mol Cell Proteomics* **9:** 271–284.

Frey BJ, Dueck D. 2007. Clustering by passing messages between data points. *Science* **315**: 972-976.

Giniger E, Tietje K, Jan LY, Jan YN. 1994. lola encodes a putative transcription factor required for axon growth and guidance in *Drosophila*, *Development* **120:** 1385–1398.

Gonsalves SE, Neal SJ, Kehoe AS, Westwood JT. 2011. Genome-wide examination of the transcriptional response to ecdysteroids 20-hydroxyecdysone and ponasterone A in *Drosophila* melanogaster, *BMC Genomics* **12:** 475.

Graveley BR, Brooks AN, Carlson JW, Duff MO, Landolin JM, Yang L, Artieri CG, van Baren MJ, Boley N, Booth BW, et al. 2011. The developmental transcriptome of *Drosophila* melanogaster, *Nature* **471:** 473–479.

Griffin TJ, Gygi SP, Ideker T, Rist B, Eng J, Hood L, Aebersold R. 2002. Complementary profiling of gene expression at the transcriptome and proteome levels in Saccharomyces cerevisiae, *Mol Cell Proteomics* **1:** 323–333.

Grün D, Kirchner M, Thierfelder N, Stoeckius M, Selbach M, Rajewsky N. 2014. Conservation of mRNA and protein expression during development of C. elegans, *Cell Rep* **6:** 565–577.

Harrison PM, Milburn D, Zhang Z, Bertone P, Gerstein M. 2003. Identification of pseudogenes in the *Drosophila* melanogaster genome, *Nucleic Acids Res* **31:** 1033–1037.

Jambor H, Surendranath V, Kalinka AT, Mejstrik P, Saalfeld S, Tomancak P. 2015. Systematic imaging reveals features and changing localization of mRNAs in *Drosophila* development, *Elife* **4**.

Kalinka AT, Varga KM, Gerrard DT, Preibisch S, Corcoran DL, Jarrells J, Ohler U, Bergman CM, Tomancak P. 2010. Gene expression divergence recapitulates the developmental hourglass model, *Nature* **468:** 811–814.

Kappei D, Butter F, Benda C, Scheibe M, Draskovic I, Stevense M, Novo CL, Basquin C, Araki M, Araki K, et al. 2013. HOT1 is a mammalian direct telomere repeat-binding protein contributing to telomerase recruitment, *EMBO J* **32:** 1681–1701.

Kharchenko PV, Alekseyenko AA, Schwartz YB, Minoda A, Riddle NC, Ernst J, Sabo PJ, Larschan E, Gorchakov AA, Gu T, et al. 2011. Comprehensive analysis of the chromatin landscape in *Drosophila* melanogaster, *Nature* **471:** 480–485.

Kondo S, Ueda R. 2013. Highly improved gene targeting by germline-specific Cas9 expression in *Drosophila*, *Genetics* **195:** 715–721.

Kooperberg. 2016 logspline: Logspline Density Estimation Routines. https://CRAN.R-project.org/package=logspline

Kronja I, Whitfield ZJ, Yuan B, Dzeyk K, Kirkpatrick J, Krijgsveld J, Orr-Weaver TL. 2014. Quantitative proteomics reveals the dynamics of protein changes during *Drosophila* oocyte maturation and the oocyte-to-embryo transition, *Proc Natl Acad Sci U S A* **111:** 16023–16028.

Ladoukakis E, Pereira V, Magny EG, Eyre-Walker A, Couso JP. 2011. Hundreds of putatively functional small open reading frames in *Drosophila*, *Genome Biol* **12:** R118.

Lawrence PA. 1992. *The making of a fly. The genetics of animal design / Peter A. Lawrence*. Blackwell Scientific, Oxford.

Lécuyer E, Yoshida H, Parthasarathy N, Alm C, Babak T, Cerovina T, Hughes TR, Tomancak P, Krause HM. 2007. Global analysis of mRNA localization reveals a prominent role in organizing cellular architecture and function, *Cell* **131:** 174–187.

Liu N, Lasko P. 2015. Analysis of RNA Interference Lines Identifies New Functions of Maternally-Expressed Genes Involved in Embryonic Patterning in *Drosophila* melanogaster, *G3 (Bethesda)* **5:** 1025–1034.

Liu Y, Beyer A, Aebersold R. 2016. On the Dependency of Cellular Protein Levels on mRNA Abundance, *Cell* **165:** 535–550.

Luschnig S, Moussian B, Krauss J, Desjeux I, Perkovic J, Nüsslein-Volhard C. 2004. An F1 genetic screen for maternal-effect mutations affecting embryonic pattern formation in *Drosophila* melanogaster, *Genetics* **167:** 325–342.

Magny EG, Pueyo JI, Pearl FMG, Cespedes MA, Niven JE, Bishop SA, Couso JP. 2013. Conserved regulation of cardiac calcium uptake by peptides encoded in small open reading frames, *Science* **341:** 1116–1120.

Mani SR, Megosh H, Lin H. 2014. PIWI proteins are essential for early *Drosophila* embryogenesis, *Dev Biol* **385:** 340–349.

Margolin W. 2012. The price of tags in protein localization studies, *J Bacteriol* **194:** 6369–6371.

Matthews BB, Dos Santos G, Crosby MA, Emmert DB, St Pierre SE, Gramates LS, Zhou P, Schroeder AJ, Falls K, Strelets V, et al. 2015. Gene Model Annotations for *Drosophila* melanogaster: Impact of High-Throughput Data, *G3 (Bethesda)* **5:** 1721–1736.

McGraw LA, Clark AG, Wolfner MF. 2008. Post-mating gene expression profiles of female *Drosophila* melanogaster in response to time and to four male accessory gland proteins, *Genetics* **179:** 1395–1408.

Morin X, Daneman R, Zavortink M, Chia W. 2001. A protein trap strategy to detect GFP-tagged proteins expressed from their endogenous loci in *Drosophila*, *Proc Natl Acad Sci U S A* **98:** 15050–15055.

Nagarkar-Jaiswal S, Lee P-T, Campbell ME, Chen K, Anguiano-Zarate S, Gutierrez MC, Busby T, Lin W-W, He Y, Schulze KL, et al. 2015. A library of MiMICs allows tagging of genes and reversible, spatial and temporal knockdown of proteins in *Drosophila*, *Elife* **4**.

Peshkin L, Wühr M, Pearl E, Haas W, Freeman RM, Gerhart JC, Klein AM, Horb M, Gygi SP, Kirschner MW. 2015. On the Relationship of Protein and mRNA Dynamics in Vertebrate Embryonic Development, *Dev Cell* **35:** 383–394.

R Core Team. 2017. R: A language and environment for statistical computing. R Foundation for Statistical Computing, Vienna, Austria. https://www.R-project.org/.

Ramamurthi KS, Storz G. 2014. The small protein floodgates are opening; now the functional analysis begins, *BMC Biol* **12:** 96.

Sandmann T, Jensen LJ, Jakobsen JS, Karzynski MM, Eichenlaub MP, Bork P, Furlong EEM. 2006. A temporal map of transcription factor activity: mef2 directly regulates target genes at all stages of muscle development, *Dev Cell* **10:** 797–807.

Sarov M, Barz C, Jambor H, Hein MY, Schmied C, Suchold D, Stender B, Janosch S, Kj VV, Krishnan RT, et al. 2016. A genome-wide resource for the analysis of protein localisation in *Drosophila*, *Elife* **5**.

Schwanhäusser B, Busse D, Li N, Dittmar G, Schuchhardt J, Wolf J, Chen W, Selbach M. 2011. Global quantification of mammalian gene expression control, *Nature* **473:** 337–342.

Simmons MJ, Thorp MW, Buschette JT, Peterson K, Cross EW, Bjorklund EL. 2010. Maternal impairment of transposon regulation in *Drosophila* melanogaster by mutations in the genes aubergine, piwi and Suppressor of variegation 205, *Genet Res (Camb)* **92:** 261–272.

Sowell RA, Hersberger KE, Kaufman TC, Clemmer DE. 2007. Examining the proteome of *Drosophila* across organism lifespan, *J Proteome Res* **6:** 3637–3647.

Sury MD, Chen J-X, Selbach M. 2010. The SILAC fly allows for accurate protein quantification in vivo, *Mol Cell Proteomics* **9:** 2173–2183.

Tadros W, Lipshitz HD. 2005. Setting the stage for development: mRNA translation and stability during oocyte maturation and egg activation in *Drosophila*, *Dev Dyn* **232:** 593–608.

Takemori N, Yamamoto M-T. 2009. Proteome mapping of the *Drosophila* melanogaster male reproductive system, *Proteomics* **9:** 2484–2493.

The modENCODE consortium, Roy S, Ernst J, Kharchenko PV, Kheradpour P, Negre N, Eaton ML, Landolin JM, Bristow CA, Ma L, Lin MF, et al. 2010. Identification of functional elements and regulatory circuits by *Drosophila* modENCODE, *Science* **330:** 1787–1797.

Tomancak P, Berman BP, Beaton A, Weiszmann R, Kwan E, Hartenstein V, Celniker SE, Rubin GM. 2007. Global analysis of patterns of gene expression during *Drosophila* embryogenesis, *Genome Biol* **8:** R145.

Vogel C, Marcotte EM. 2012. Insights into the regulation of protein abundance from proteomic and transcriptomic analyses, *Nat Rev Genet* **13:** 227–232.

Wasbrough ER, Dorus S, Hester S, Howard-Murkin J, Lilley K, Wilkin E, Polpitiya A, Petritis K, Karr TL. 2010. The *Drosophila* melanogaster sperm proteome-II (DmSP-II), *J Proteomics* **73:** 2171–2185.

Xing X, Zhang C, Li N, Zhai L, Zhu Y, Yang X, Xu P. 2014. Qualitative and quantitative analysis of the adult *Drosophila* melanogaster proteome, *Proteomics* **14:** 286–290.

Yamanaka N, Rewitz KF, O'Connor MB. 2013. Ecdysone control of developmental transitions: lessons from *Drosophila* research, *Annu Rev Entomol* **58:** 497–516.

FIGURE LEGENDS

Fig. 1. ***Drosophila*** **developmental life cycle proteome.**

(A) Scheme depicting the collected time points throughout the four major metamorphic stages of *Drosophila* (embryo [red], larva [blue], pupa [green] and adult [violet]). WP: white pupa, L3c: crawling third instar larva. (B) Heat map of $\log_2$ LFQ values of the 7,952 protein groups quantified during fly development. (C) Visualization of the first two principal components separating samples according to their developmental stage. The biological replicates are indicated in the same color with elliptic areas representing the standard error of the two depicted components.

Fig. 2. Characteristics of the developmental proteome.

(A) Overlap of quantified protein groups between developmental stages results in a core proteome of 4,627 proteins. (B) Clusters of enriched GO terms obtained from the core proteome are plotted in a coordinate system defined by the first two dimensions of a multidimensional scaling according to their similarity scores. The color of the circle represents the GO cluster with a representative term highlighted. The diameter of the circle is proportional to the size of the GO category. (C) The density plot relates protein abundance with a dynamicity score during developmental protein expression (log_{10} transformed Gini index). In the lower-right quadrant, highly stable proteins are represented, while the upper-right quadrant contains proteins with changing expression levels during development. (D) Expression profiles for two highly dynamic (upper panel) and two stably expressed (lower panel) proteins highlighted in red in the dynamicity plot.

Fig. 3. Stage-specific proteins and ecdysone-induced developmental regulation.

(A) Heat map showing 1,535 protein groups found to be differentially (ANOVA, FDR<0.01) regulated during the life cycle. These protein groups were clustered into up to 12 stage-specific profiles. Average profiles of the individual clusters for each developmental stage are shown. B) Heat map showing log_2 LFQ abundance of proteins with stage-specific expression profiles discussed in the text. (C) Schematic representation of ecdysone pulses during fly development (upper panel) and heat map of log_2 LFQ expression levels of selected proteins of 20-hydroxyecdysone regulated genes (lower panel). (D) For the *Eig71E* and *Sgs* gene family, RNA expression profiles (dotted line) differ from protein levels (solid line) during the pupal phase demonstrating prolonged protein stability. (E) Three examples showing single protein expression burst, but more broadly detectable RNA indicating more tightly controlled protein expression.

Fig. 4. Gender-specific proteome and maternally loaded proteins.

(A) Volcano plot comparing protein expression levels between one-week-old male and female flies. Candidates discussed in the text are highlighted (filled black circle). Dashed lines indicate a 4-fold expression difference with $p<0.01$. (B) Volcano plot comparing protein expression levels between young male and female flies (less than 4 hours old after eclosure) shows very few female-specific proteins. Candidates discussed in the text are highlighted (filled black circle). Dashed lines indicate a 4-fold expression difference with $p<0.01$. (C) Developmental expression profile of the female-specific protein CG31862 shows detection of mRNA (dotted line) in late pupal stage, while the protein (solid line) is also found in female flies. (D) Integration of mRNA levels with embryo-specific proteins allows identifying maternally loaded proteins. The mRNA levels of the adult female flies compared to embryos (x-axis) and males (y-axis) distinguishes cases in which either both, the mRNA and protein ($x=0$, $y>2$) or only the protein (darker shaded area) is maternally loaded. (E) Relative embryonic hatching rate (four biological replicates) of *CG17018* knockdown embryos compared to wild type. (F) Image of representative wild type and the *CG17018* knockdown embryo with fused dorsal appendages. (G) Cuticle preparation of embryos revealed absence of denticle belts patterning in the *CG17018* knockdown line.

Fig. 5. Small proteins and peptides from non-coding regions of the genome.

(A) Protein length distribution of identified (green, not enough quantitation values) and quantified (orange) protein groups of the life cycle proteome. Most proteins have quantitation values (>90 percent) and this fraction only marginally depends on protein length. The red line demarcates the fraction of 268 small proteins (<100 aa). (B) Representative MS/MS spectrum with annotated b- and y-ions of the peptide INILKSVNK$^{(2+)}$ from the putative non-coding gene *CR43476*. (C) Sequence comparison of Cyp9f2 and the “pseudogene” product Cyp9f3psi with amino acid substitution between both proteins marked in orange. Coverage of peptides for either protein is shown (yellow, more intense regions have overlapping peptides).

Fig. 6. The embryogenesis proteome time course.

(A) Scheme indicating the collected time points. PCA shows high reproducibility of replicates and the first component shows high correlation with developmental progression (R=0.93). (B) Heat map of $\log_2$ LFQ expression values for 1,644 developmentally regulated protein groups in embryogenesis. (C) Western blots of seven selected proteins validate their temporal expression profile from the proteomics screen. (D) Dot plot connecting the selected enriched GO terms with developmental progression. The circle size indicates the odds ratio of each GO term category. (E) The regulated protein groups have been assigned automatically to 70 clusters based on expression profiles of which four representative clusters with an upregulation at 2-3h (cluster 41), 5h (cluster 10), 10h (cluster 60) and 20h (cluster 57) are shown. (F) Profiles of tissue-specific protein expression created by integrating RNA fluorescence *in situ* hybridization data. Muscle and central nervous system (CNS) clusters were chosen as examples. (G) Ubiquitous (*tubulin*-GAL4) and mesodermal (*24B*- and *mef2*-GAL4), but not neuronal (*elav-GAL4*) knockdown of *CG1674* results in reduced locomotion activity (Dunnett's test; *** p-value <0.001).

Fig. 7. Temporal transcriptome/proteome dynamics and isoform quantitation.

(A) Plot showing the number (bars) of detected transcripts (orange) and proteins (green) at each time point. The solid line depicts the cumulative sum of unique transcripts (orange) and proteins (green). The dashed line represents the median across all time points. (B) Heat map displaying the Pearson correlation between transcript and protein expression levels. Matching time points between the two datasets are indicated by orange boxes. (C) Median scaled quantification plotted after clustering of the first PCA component of RNA (orange) and protein (green) expression into six different categories. Shaded regions display the standard error of the fitted line. (D) Expression profiles with isoforms-specific information of three proteins: Lola, Mod(mdg4) and Rtnl1. Isoforms are colored according to the legend. (E) Validation of Lola-RAA/Lola-RI isoform quantitation by immunoblotting against Lola at four selected time points.

Protein lysate of *lola*-RAA/*lola*-RI mutant embryos at 20h were used to identify the isoform-specific band (arrow) corresponding to Lola-RAA/Lola-RI. Beta-tubulin was used as a loading control. (F) RNA levels were determined by *in situ* hybridization at the selected time points with a specific probe for *lola*-RAA/*lola*-RI.

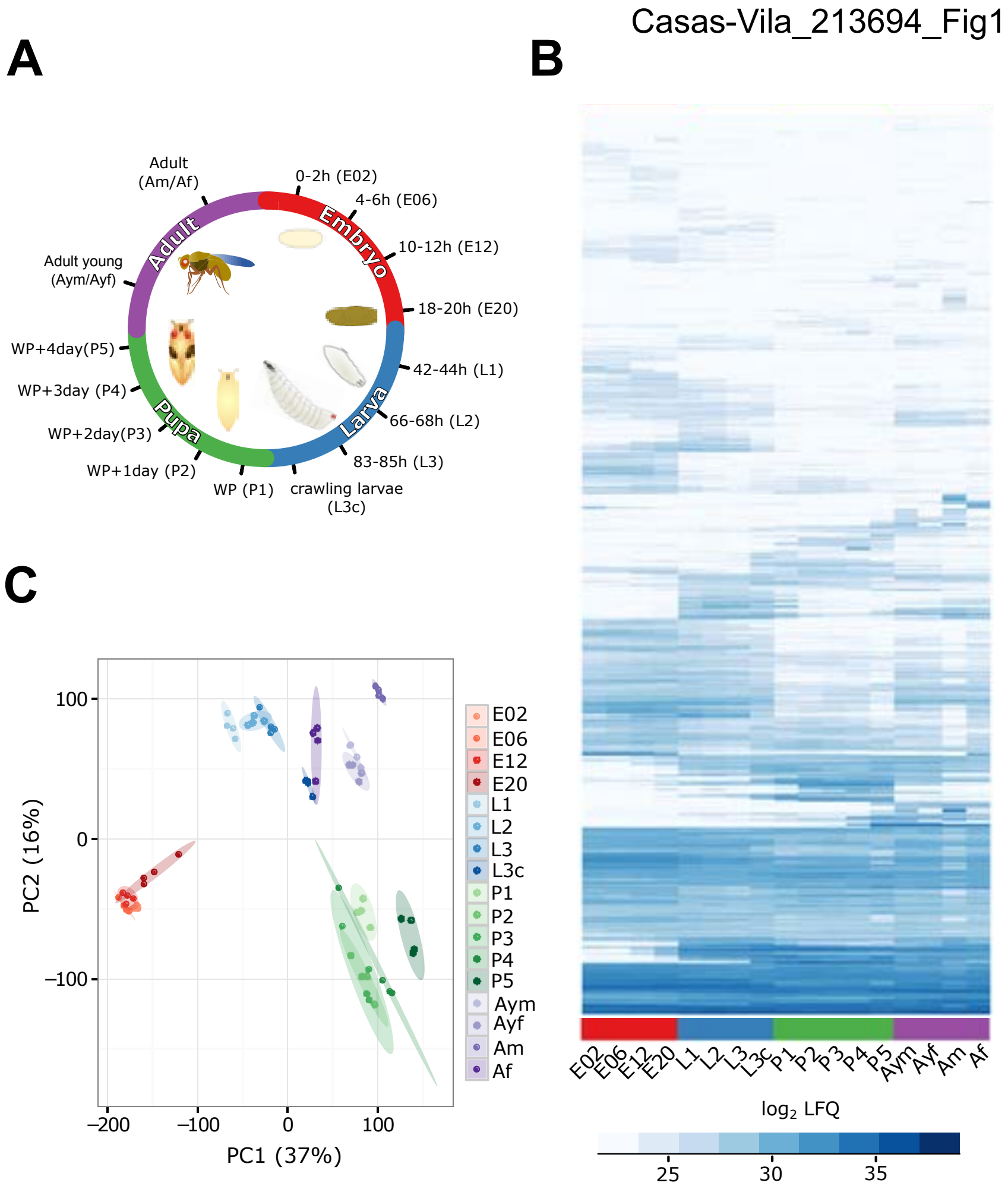
A
Adult
(Am/Af)
0-2h (E02)
4-6h (E06)
10-12h (E12)
18-20h (E20)
42-44h (L1)
66-68h (L2)
83-85h (L3)
crawling larvae
(L3c)
WP (P1)
WP+1day (P2)
WP+2day(P3)
WP+3day (P4)
WP+4day(P5)
Adult young
(Aym/Ayf)
Adult
Embryo
Larva
Pupa
B
E02
E06
E12
E20
L1
L2
L3
L3c
P1
P2
P3
P4
P5
Aym
Ayf
Am
Af
log2 LFQ
25
30
35
C
100
0
−100
−200
−100
0
100
PC1 (37%)
PC2 (16%)
E02
E06
E12
E20
L1
L2
L3
L3c
P1
P2
P3
P4
P5
Aym
Ayf
Am
Af

Casas-Vila_213694_Fig2

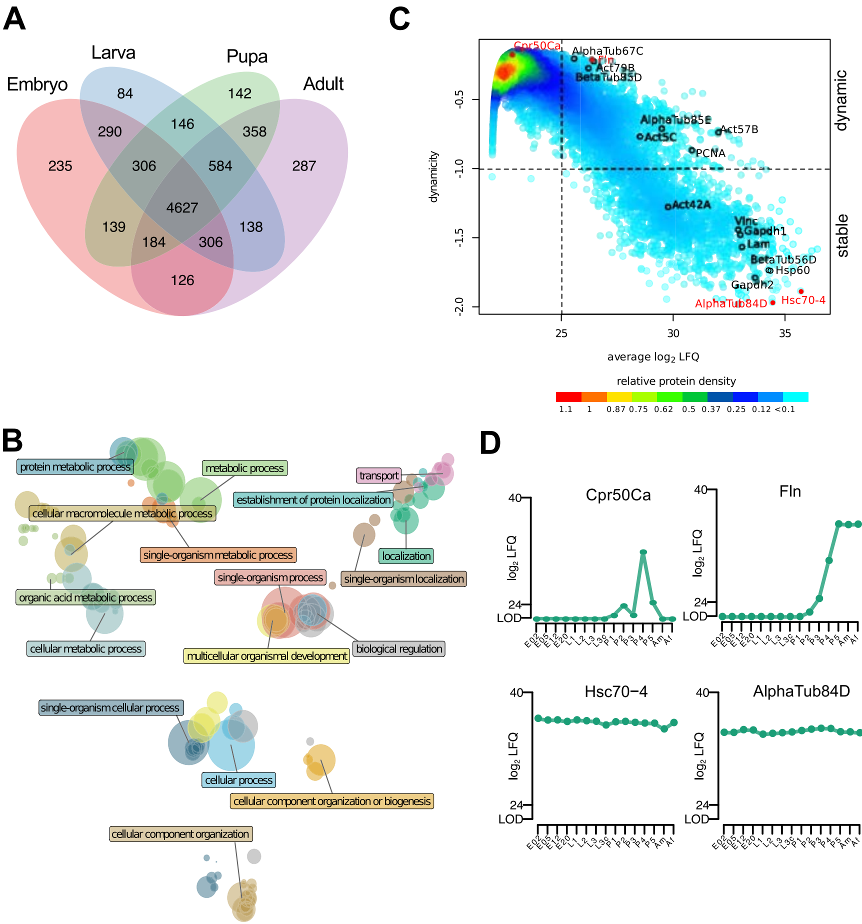

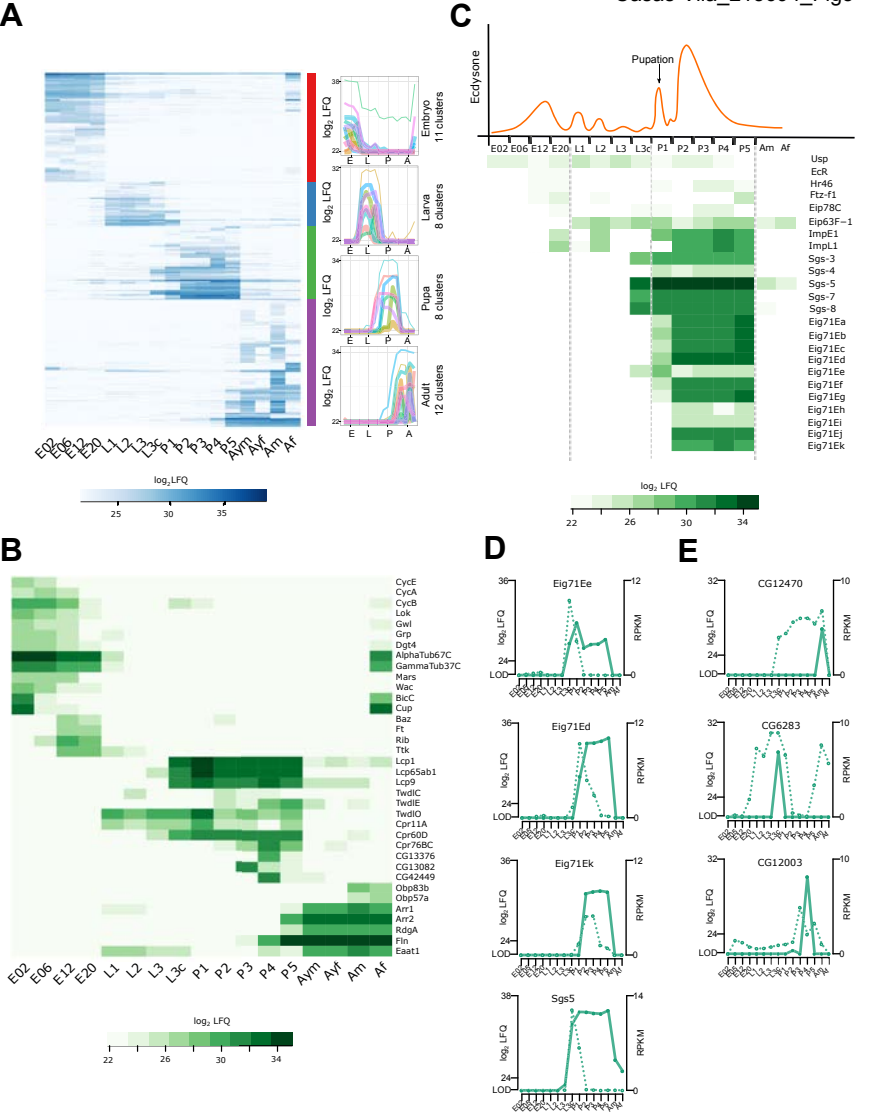
A
log2 LFQ
Embryo
11 clusters
Larva
8 clusters
Pupa
8 clusters
Adult
12 clusters
E L P A
E02 E06 E12 E20 L1 L2 L3 L3c P1 P2 P3 P4 P5 Aym Avf Am Af
log2 LFQ
25 30 35
B
CycE
CycA
CycB
Lok
Gwl
Grp
Dgt4
AlphaTub67C
GammaTub37C
Mars
Wac
BicC
Cup
Baz
Ft
Rib
Ttk
Lcp1
Lcp65ab1
Lcp9
TwdlC
TwdlE
TwdlO
Cpr11A
Cpr60D
Cpr76BC
CG13376
CG13082
CG42449
Obp83b
Obp57a
Arr1
Arr2
RdgA
Fln
Eaat1
E02 E06 E12 E20 L1 L2 L3 L3c P1 P2 P3 P4 P5 Aym Avf Am Af
log2 LFQ
22 26 30 34
C
Ecdysone
Pupation
E02 E06 E12 E20 L1 L2 L3 L3c P1 P2 P3 P4 P5 Am Af
Usp
EcR
Hr46
Ftz-f1
Eip78C
Eip63F−1
ImpE1
ImpL1
Sgs-3
Sgs-4
Sgs-5
Sgs-7
Sgs-8
Eig71Ea
Eig71Eb
Eig71Ec
Eig71Ed
Eig71Ee
Eig71Ef
Eig71Eg
Eig71Eh
Eig71Ei
Eig71Ej
Eig71Ek
log2 LFQ
22 26 30 34
D
Eig71Ee
Eig71Ed
Eig71Ek
Sgs5
log2 LFQ
RPKM
LOD
E
CG12470
CG6283
CG12003
log2 LFQ
RPKM
LOD

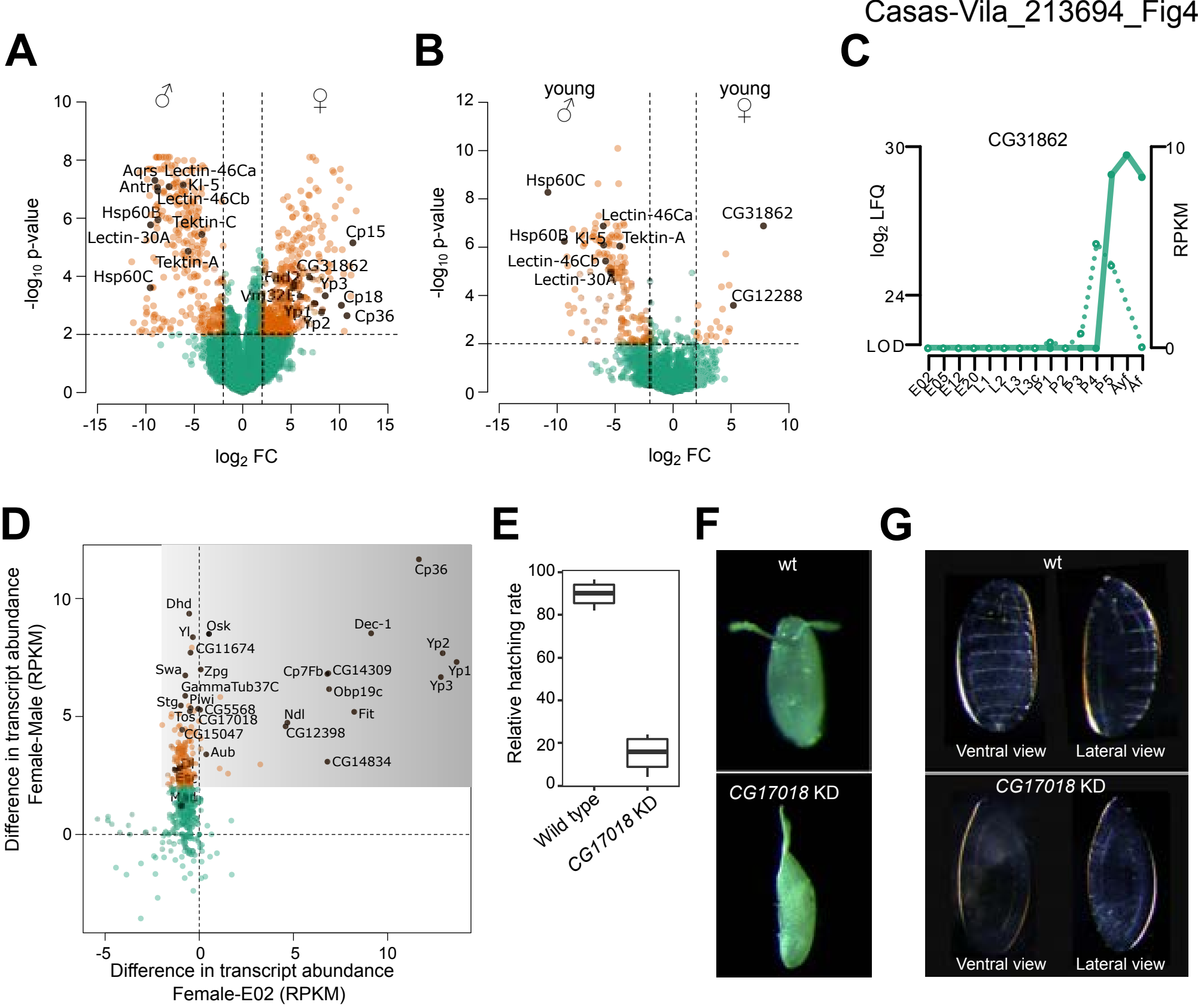
A
B
C
D
E
F
G
-log10 p-value
log2 FC
young
Aqrs
Lectin-46Ca
Antr
Kl-5
Lectin-46Cb
Hsp60B
Tektin-C
Lectin-30A
Cp15
Tektin-A
CG31862
Hsp60C
Ndl2
Yp3
Vm37Fb
Cp18
Yp1
Cp36
Yp2
Tektin-A
CG12288
log2 LFQ
RPKM
LOD
E02
E05
E12
E20
L1
L2
L3
L3c
P1
P2
P3
P4
P5
Avf
Af
Difference in transcript abundance Female-Male (RPKM)
Difference in transcript abundance Female-E02 (RPKM)
Dhd
Yl
Osk
CG11674
Dec-1
Swa
Zpg
Cp7Fb
CG14309
GammaTub37C
Obp19c
Stg
Piwi
CG5568
Tos
CG17018
Ndl
Fit
CG15047
CG12398
Aub
CG14834
Relative hatching rate
Wild type
CG17018 KD
wt
Ventral view
Lateral view

Casas-Vila_213694_Fig5

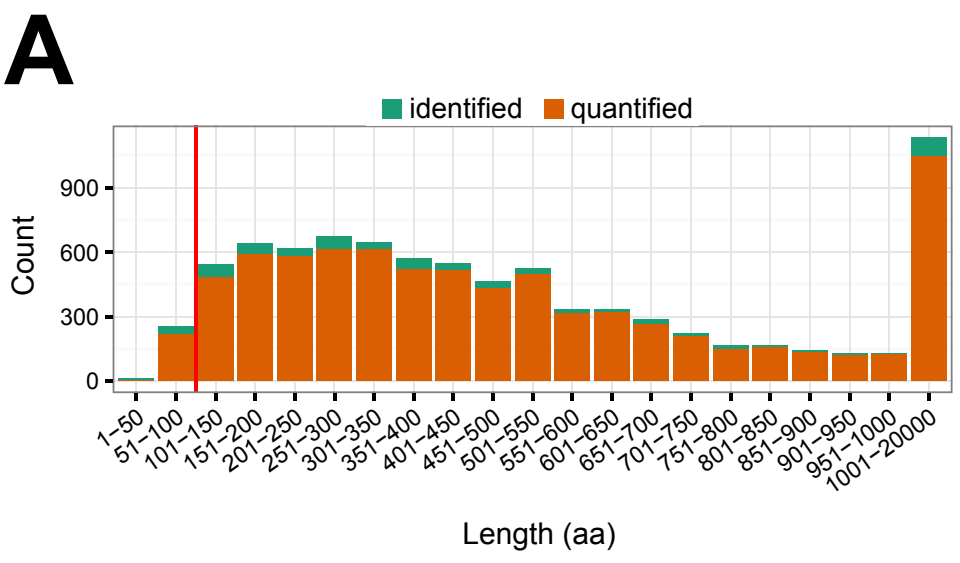

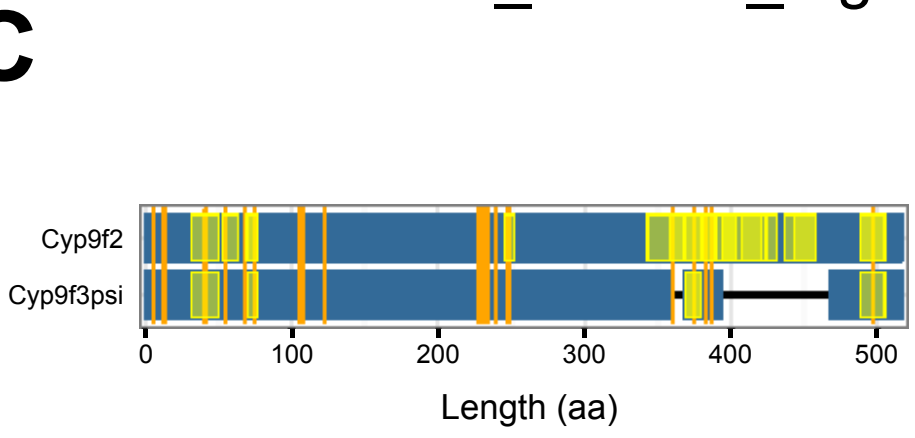

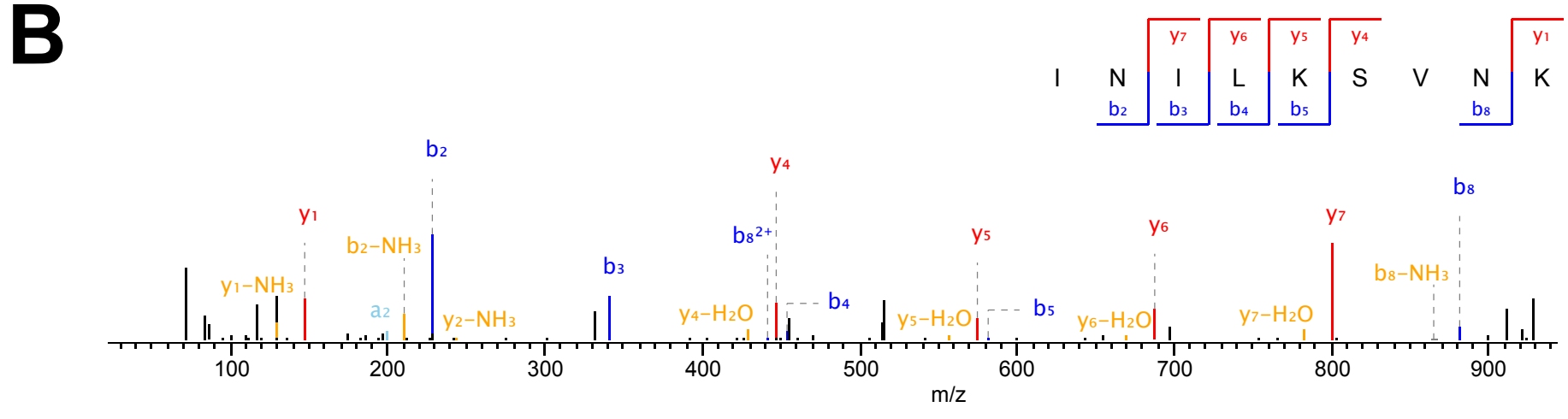

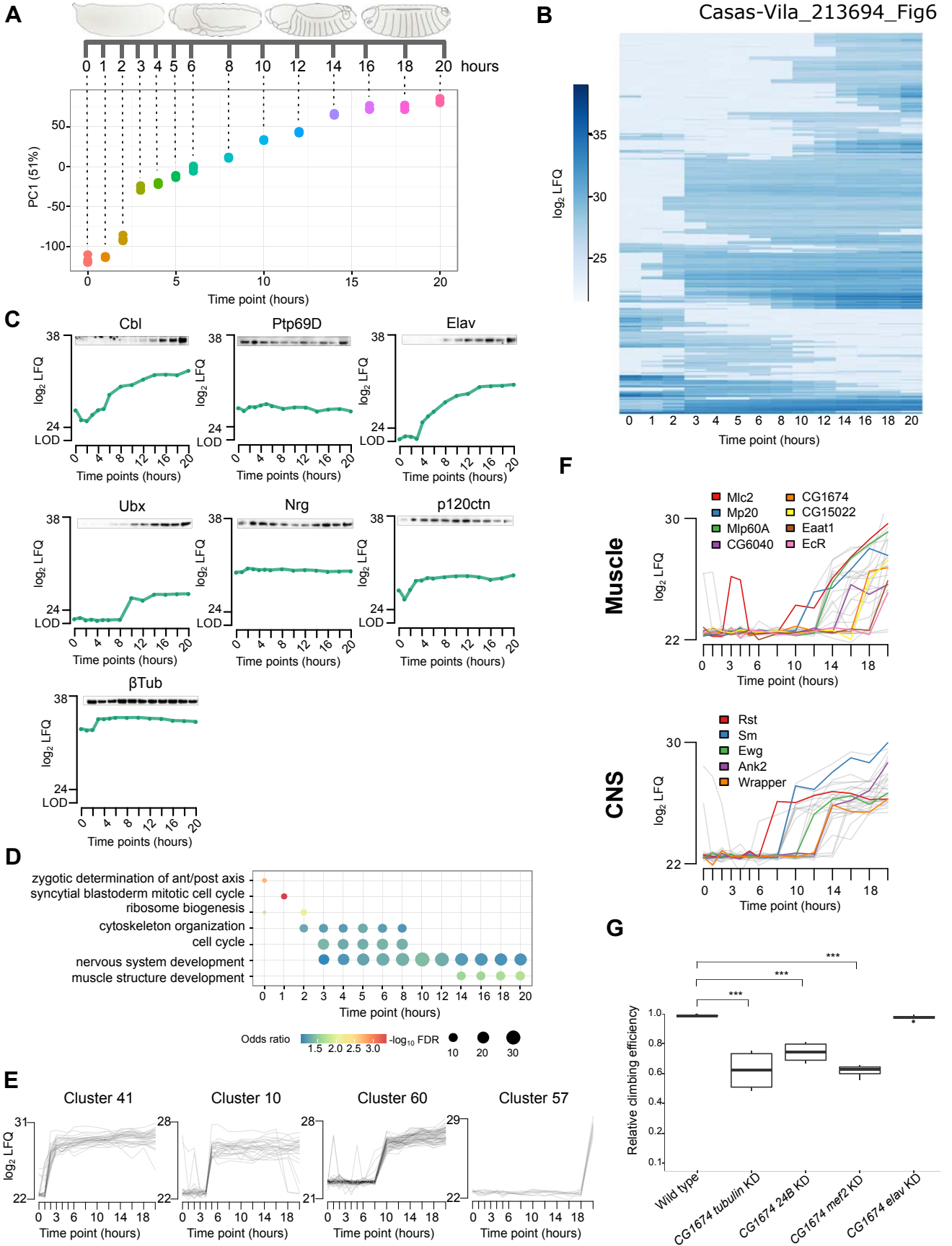
A
0 1 2 3 4 5 6 8 10 12 14 16 18 20 hours
PC1 (51%)
Time point (hours)
B
Casas-Vila_213694_Fig6
log2 LFQ
Time point (hours)
C
Cbl
Ptp69D
Elav
Ubx
Nrg
p120ctn
βTub
log2 LFQ
LOD
Time points (hours)
D
zygotic determination of ant/post axis
syncytial blastoderm mitotic cell cycle
ribosome biogenesis
cytoskeleton organization
cell cycle
nervous system development
muscle structure development
Time point (hours)
Odds ratio
-log10 FDR
E
Cluster 41
Cluster 10
Cluster 60
Cluster 57
log2 LFQ
Time point (hours)
F
Muscle
Mlc2
Mp20
Mlp60A
CG6040
CG1674
CG15022
Eaat1
EcR
CNS
Rst
Sm
Ewg
Ank2
Wrapper
log2 LFQ
Time point (hours)
G
Relative climbing efficiency
***
Wild type
CG1674 tubulin KD
CG1674 24B KD
CG1674 mef2 KD
CG1674 elav KD

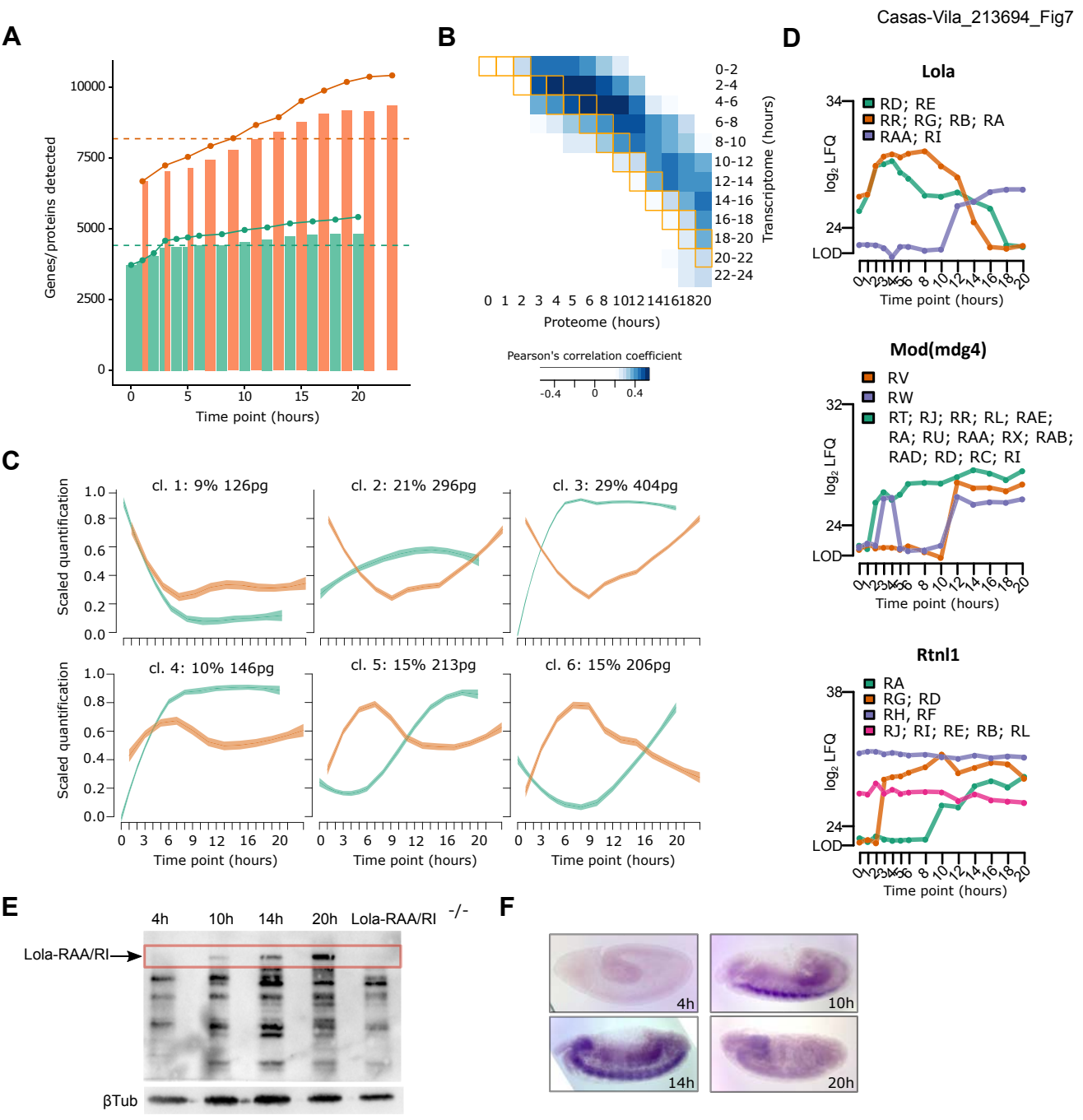
A
Genes/proteins detected
Time point (hours)
B
Transcriptome (hours)
Proteome (hours)
Pearson's correlation coefficient
D
Lola
RD; RE
RR; RG; RB; RA
RAA; RI
log2 LFQ
LOD
Time point (hours)
Mod(mdg4)
RV
RW
RT; RJ; RR; RL; RAE; RA; RU; RAA; RX; RAB; RAD; RD; RC; RI
Rtnl1
RA
RG; RD
RH, RF
RJ; RI; RE; RB; RL
C
cl. 1: 9% 126pg
cl. 2: 21% 296pg
cl. 3: 29% 404pg
cl. 4: 10% 146pg
cl. 5: 15% 213pg
cl. 6: 15% 206pg
Scaled quantification
Time point (hours)
E
4h
10h
14h
20h
Lola-RAA/RI
-/-
βTub
F
4h
10h
14h
20h